Rapid disorganization of mechanically interacting systems of mammary acini

Quanming Shi[a,b,1], Rajarshi P. Ghosh[a,b,1], Hanna Engelke[a,b], Chris H. Rycroft[a,c,d], Luke Cassereau[a,e], James A. Sethian[a,c,d], Valerie M. Weaver[a,e,2], and Jan T. Liphardt[a,b,2]

[a]Bay Area Physical Sciences Oncology Center and Departments of [b]Physics and [c]Mathematics, University of California, Berkeley, CA 94720; [d]Mathematics Department, Lawrence Berkeley National Laboratory, Berkeley, CA 94720; and [e]Departments of Surgery, Anatomy, Bioengineering, Therapeutic Sciences, and Center for Bioengineering and Tissue Regeneration, University of California, San Francisco, CA 94143

Edited by José N. Onuchic, Rice University, Houston, TX, and approved November 4, 2013 (received for review June 18, 2013)

Cells and multicellular structures can mechanically align and concentrate fibers in their ECM environment and can sense and respond to mechanical cues by differentiating, branching, or disorganizing. Here we show that mammary acini with compromised structural integrity can interconnect by forming long collagen lines. These collagen lines then coordinate and accelerate transition to an invasive phenotype. Interacting acini begin to disorganize within 12.5 ± 4.7 h in a spatially coordinated manner, whereas acini that do not interact mechanically with other acini disorganize more slowly (in 21.8 ± 4.1 h) and to a lesser extent ($P < 0.0001$). When the directed mechanical connections between acini were cut with a laser, the acini reverted to a slowly disorganizing phenotype. When acini were fully mechanically isolated from other acini and also from the bulk gel by box-cuts with a side length <900 μm, transition to an invasive phenotype was blocked in 20 of 20 experiments, regardless of waiting time. Thus, pairs or groups of mammary acini can interact mechanically over long distances through the collagen matrix, and these directed mechanical interactions facilitate transition to an invasive phenotype.

mechanobiology | cancer

Epithelial cells are physically coupled to their neighbors and are also in contact with the ECM. The ECM confers mechanical integrity to tissues and provides chemical, anatomical, and mechanical signals to cells, influencing differentiation, development, and pathogenesis (1–11). The extent to which mechanical cues are generated and received by individual cells has been studied both experimentally and theoretically (12–14). Progress has also been made in understanding the signaling pathways that cells use to sense external mechanics. Cell-ECM interactions are mediated in part by transmembrane proteins typified by the integrins, which link the cell's internal actin cytoskeleton with extracellular collagen fibers (15). Cells use multiple approaches for integrating mechanical cues with biochemical cues provided by soluble factors; for example, there is extensive multilayered cross-talk between integrin and TGF-β signaling (16, 17). It is now also clear that key developmental regulators, such as Notch, can be directly activated by mechanical force (18, 19).

Less is known about the interactions of organized multicellular structures with the ECM and how those interactions affect tissue architecture, composition, and stability, as well as the molecular pathways by which these effects are mediated. In certain situations, contractile multicellular structures are able to mechanically reorganize biopolymer networks over long distances and in a highly directional manner, generating what are variously referred to as fibers, tracts, cables, straps, or lines. Regions of highly directional collagen alignment and concentration have been seen in systems ranging from single cells and tumor explants to human clinical samples (6, 8, 10, 20–22). Vader et al. demonstrated that the formation of long collagen lines is a mechanical phenomenon that reflects the fundamental nonlinear properties of fibrous biological networks (10). Collagen lines control the morphogenesis of epithelial tubular patterns (8) and may also influence where and when tumors invade the surrounding stroma. Indeed, regions of aligned collagen that extend radially from the tumor/stromal boundary are associated with poor outcomes in humans, in the setting of breast cancer (22). Tissue hardening due to changes in collagen cross-linking status and composition has recently even been causally implicated in tumor progression (23) and metastasis (24).

Motivated by these reports, we investigated in a model system whether contractility-induced collagen lines influence the transition to an invasive phenotype. Our model system is inspired by the anatomy of the human mammary gland, wherein tens of milk-producing mammary acini are organized into terminal duct lobular units (TDLUs) by a shared ECM. We chose Ras-transformed mammary acini as our model because most breast cancers originate in mammary acini (25), and Ras is the most frequent oncogene in human cancer (26). Our specific goal was to learn how potential mechanical cues generated by groups of genetically primed or structurally compromised acini determine the probability, timing, and extent of subsequent disorganization toward an invasive phenotype.

Results and Discussion

We extracted 8-d-old Ras-transformed MCF10AT mammary acini from 3D-reconstituted basement membrane (rBM) culture (27, 28) and washed the acini in ice-cold Tris/EDTA buffer to

Significance

Tissue mechanics are important in differentiation and development but also in diseases like breast cancer. Most breast cancers start in mammary acini, which are basic anatomical units of the mammary gland. We found in a model system that mammary acini can coordinate their disorganization toward a malignant phenotype through long-range mechanical interactions. When two or more contractile acini are sufficiently close together, they can interact via collagen lines that form between them due to acinar contractility and the nonlinearity of collagen mechanics. Disorganization of interacting acini is more probable, rapid, and extensive than that of noninteracting acini. The results may help to better understand how extrinsic factors such as tissue architecture and mechanics contribute to tumor initiation and progression.

Author contributions: Q.S., R.P.G., V.M.W., and J.T.L. designed research; Q.S., R.P.G., and J.T.L. performed research; Q.S., R.P.G., and V.M.W. contributed new reagents/analytic tools; Q.S., R.P.G., H.E., C.H.R., L.C., J.A.S., and J.T.L. analyzed data; and Q.S., R.P.G., H.E., C.H.R., J.A.S., V.M.W., and J.T.L. wrote the paper.

The authors declare no conflict of interest.

This article is a PNAS Direct Submission.

[1]Q.S. and R.P.G. contributed equally to this work.

[2]To whom correspondence may be addressed. E-mail: Valerie.Weaver@ucsfmedctr.org or jan.liphardt@stanford.edu.

This article contains supporting information online at www.pnas.org/lookup/suppl/doi:10.1073/pnas.1311312110/-/DCSupplemental.

www.pnas.org/cgi/doi/10.1073/pnas.1311312110

Downloaded at Palestinian Territory, occupied on December 9, 2021

www.manaraa.com

remove the rBM. The wash procedure was developed to preserve overall acinar morphology but to mimic conditions intrinsic to a premalignant acinus, by compromising the acinar BM, as judged by the thickness of laminin surrounding the acini, and weakening cadherin-based adherens junctions, as judged by reduction of β-catenin signal from cell-cell interfaces (Fig. S1 *A* and *B*). Thinning of the BM enables the acini to sense and engage the collagen matrix and weakening of cadherin-based adherens junctions destabilizes tissue integrity to increase lamellipodia activity (29) and actomyosin traction-driven cell scattering (30), which mirrors a genetically primed acinus that precedes transition to an invasive and metastatic tumor. Thus, treated acini deposited on rBM remained intact, as expected, because rBM supports normal development of the cells into polarized and growth-arrested structures (27, 28). However, acini allowed to settle on collagen 1 disorganized within several hours (Fig. 1 *A* and *B*), a process involving disruption of basal tissue polarity (11). The fraction of acini that disorganized depended on the duration of the Tris/EDTA wash step and the degree of disorganization depended weakly on bulk collagen concentration, consistent with previous reports (11) (Fig. S1 *C* and *D*).

To relate acinar morphology to collagen organization, we labeled the collagen with a novel reagent: photoactivatable CNA35-mEos2 collagen binding protein. This reagent can be photoactivated where and when desired, allowing collagen pulling and alignment, as well as large-scale substrate deformation to be visualized. We seeded about 200 acini on a 1-cm^2 block of 2 mg/mL collagen 1 and followed the acini-collagen system for up to 40 h (Fig. 1 *C* and *D* and Movie S1). As expected based on the previous literature (8, 10), the acini concentrated the collagen around and among them (Movies S2–S6), yielding pairs and clusters of acini interconnected by lines of intense collagen signal. By about 10 h, some of the acini began to disorganize, and by 20 h, many acini had lost their regular, spherical morphology, and single cells were leaving the acini and scattering on the collagen.

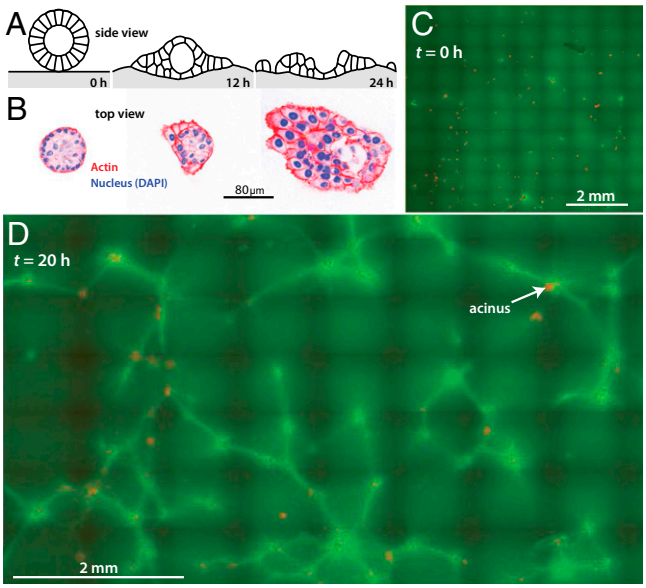

Fig. 1. Mechanical remodeling of collagen substrates by mammary acini. (*A*) Schematic of experiment. Acini are placed on collagen 1 gels and subsequent disorganization is quantified. (*B*) Acini allowed to settle on collagen gels gradually disorganize as shown by changes in acinar morphology (nuclei stained blue) and actin cytoskeleton (red). (*C*) Low-magnification overview of a system of ∼200 acini (red) on collagen 1 (green). Initially, the collagen is uniformly distributed and the acini are intact. (*D*) System of ∼200 acini after 20 h. Many acini (red) have disorganized into single cells (tiny red dots), which are scattering. The collagen has been extensively reorganized; the average green signal has dropped and bright green collagen lines run along geodesics between acini.

A closer look at the interface between collagen and acinar protrusions shows extensive alignment of the actin network among multiple cells, and in turn, this multicellular patch of aligned actin runs parallel to the adjacent extracellular collagen network, suggesting a tension generating actomyosin network acting on an elastic collagen gel (Fig. S2 and Movie S7). Indeed, the Y27632 Rho-associated protein kinase (ROCK) inhibitor (31) and the blebbistatin (32) nonmuscle myosin inhibitor significantly reduced acinar disorganization (Fig. S3). In addition, the inhibitors had a strong effect on the collagen lines. Line formation was reduced 54% by 0.5 μM blebbistatin, a concentration that is expected to reduce the ATPase rate of myosin II by only ∼10% (33). The sensitivity of the system to impairment of myosin II contractility suggests that line formation requires very high contractility. The tensions generated by the acini are transmitted to the collagen by integrins, because inhibition of focal adhesion kinase (FAK) and Src kinase by PP1 attenuated mechanical collagen remodeling (*P* values in Fig. S3).

Having confirmed the basic molecular and cellular aspects of line formation, we asked whether there was a correlation between the collagen lines and the rate of acinar disorganization. Specifically, we asked whether the presence of a directed collagen line between two acini affected their disorganization. We studied $n = 162$ contractile acini. All acini gradually concentrated the collagen and aligned it (Fig. 2 *A*–*C* and Fig. S4). Of the 162 acini, $n = 104$ interacted with other acini and $n = 58$ noninteracting acini were well separated from other acini and did not extend collagen lines to other acini. We used the acinar surface area A as our primary descriptor of acinar state; initially, acini had a mean area of $A = 0.046 \pm 0.025$ mm^2. We compared the time to disorganization for the interacting and noninteracting acini and found that interacting acini began to disorganize earlier than noninteracting acini [time to 20% area increase, 12.5 ± 4.7 (interacting) vs. 21.8 ± 4.1 h (noninteracting); two-sided t test, $P < 0.0001$], resulting in markedly distinct distribution functions in a Kaplan–Meier survival analysis, with the events defined as acinar disorganization (Fig. 2*D*; log-rank P value for difference, $P < 0.0001$). The area of interacting acini increased more rapidly than that of noninteracting acini ($P < 0.0001$). Finally, interacting acini disorganized to a greater extent than noninteracting acini [total area increase within 24 h: 1.62 ± 0.33 (interacting) vs. 1.09 ± 0.11 h (noninteracting); two-sided t test, $P < 0.0001$]. Therefore, mechanically interacting acini disorganize earlier, faster, and to a greater extent than noninteracting acini. These conclusions are robust toward changes of event definition, such as use of other morphological features, for example, sphericity to follow disorganization, or use of a phenotypic metric, such as the time to onset of cell streaming [22.1 ± 9.3 (interacting) vs. 35.0 ± 7.3 h (noninteracting); Fig. S5].

Next, we asked whether the dynamics of line formation, rather than binary presence or absence of a line connecting two acini, were correlated with the dynamics of acinar disorganization. Acini began to mechanically remodel their matrix at t ∼3 h (Fig. 2 *E* and *F*), lines formed when contractile acini were within about 1.2 mm of one another, and thus interacting acini began to spread as early as $t = 5$ h. Two of 58 noninteracting acini (Fig. 2*E*, stars) also disorganized rapidly despite not visibly interacting with other acini through the collagen substrate; we attribute those two exceptions to the presence of one or more nearby contractile acini that are outside of the imaging region of interest. The ability of interacting acini to contract their substrate was inherently self-limiting, because the acini began to scatter at t >10 h (which necessarily reduces acinar contractility; note plateau of collagen velocity at $t = 7$–11 h; Fig. 2*F*, dashed line), and in some very rare cases, the interacinar tensions were high enough to tear the collagen line (Movie S8, lower left corner),

Downloaded at Palestinian Territory, occupied on December 9, 2021
www.manaraa.com

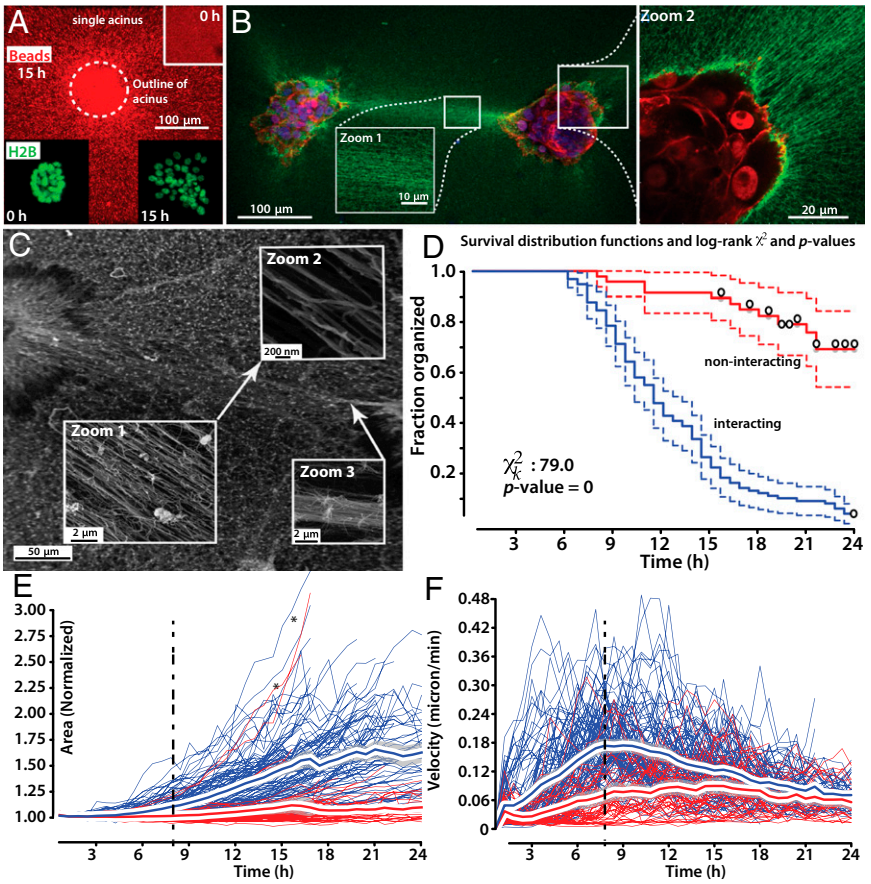

Fig. 2. Acceleration of disorganization in interacting acini. (*A*) Acini pull collagen radially inward, as shown by gradual bead enrichment near and under the acini. (Scale bar, 100 μm.) (*Inset*) Initial bead distribution. (*B*) Two acini interacting via a collagen line (green). Zoom 1, detail of collagen alignment in line. Zoom 2, detail of acinus (nuclei, red) and radially aligned collagen (green). (*C*) SEM image of collagen ultrastructure between interacting acini. Zoom 1–2, higher magnifications of aligned fibers comprising collagen line. Zoom 3, aligned collagen fibers can coalesce into higher order collagen bundle. (*D*) Survival analysis using Kaplan–Meier curves and the log-rank test show that interacting acini (blue) disorganize more rapidly than noninteracting acini (red). (*E*) Change of area of interacting (blue) and noninteracting (red) contractile acini. Interacting acini spread more rapidly than noninteracting acini (significantly different with $P < 0.001$ for $t > 4$ h) but note two exceptions (black stars), consisting of rapidly disorganizing noninteracting acini. Red line, mean; Gray shaded region, 95% CI. (*F*) Local collagen velocity near interacting (blue) and noninteracting (red) contractile acini. Velocities are significantly different with $P < 0.001$ for $1 < t < 13$ h.

which immediately reduces the tensions within the material. Interacinar interaction resulted in more rapid collagen pulling visualized by embedded bead movements compared with noninteracting acini ($P < 0.001$ between 3 and 13 h; Fig. 2*F*). Indeed, the rapidity of early bead pulling was weakly correlated ($r \sim 0.35$) with the time at which cells began to stream from an acinus (ANOVA *P* value for interacting acini: $P = 0.00059$; Fig. S6*A*), despite cell streaming occurring many hours after the time of maximum bead pulling. Interacting acini disorganized in a spatially correlated manner, because their protrusions pointed toward one another (Movies S8–S12), and on disorganization, the majority of cells and cell aggregates streamed along the collagen line from one acinus toward its partner(s) (Fig. S6*B* and Movies S9, S11, and S12). For example, as shown in Movie S12, at frame 00:29, 24 of 28 streaming cells are moving along lines connecting acini. Therefore, interacting acini manipulate the collagen in a manner that is quantifiably distinct from noninteracting acini, and these differences are correlated with phenotypic differences at the acinar level, such as morphology and the rapidity with which an invasive phenotype is seen.

These experiments suggested a connection between collagen lines and rapid acinar disorganization, but a statistical analysis does not address causality. We therefore used a UV laser to cut deep grooves into the gel, severing specific collagen lines (Fig. 3*A*, dashed white line), inspired by the use of UV lasers to study and alter the mechanics in developing fly embryos (34, 35). Laser cutting of the collagen was performed at distances of >300 μm from any acini to avoid potential phototoxicity. On severing the interconnecting collagen line between acini (Fig. 3*A*), they still disorganized, but more slowly and without directional bias. Although the simple line cut as shown in Fig. 3*A* reduced the rate of disorganization and directional preference, some interacting acini were able to ultimately bypass the defect in the gel and reconnect by new lines, which then ran along the geometrically shortest path around the cut region (Fig. 3*B*, arrows, gap bypass). We therefore turned to a different cutting geometry, in which the acini are fully mechanically isolated from other acini and the rest of the gel via a complete box cut with a side half-length *r* of 0.30 mm (Fig. 3 *C* and *D*). After being isolated by a box cut, the acini remained contractile but, strikingly, did not spread or scatter at all: 20 of 20 acini remained intact even after a waiting period of $t = 40$ h. The mechanically isolated acini were still markedly contractile, as seen by a bright ring of concentrated collagen that formed around them (Fig. 3*D*, arrow) but they did not spread or scatter. This lack of spreading or scattering is surprising because the mechanically isolated acini concentrated the collagen more than noninteracting or interacting acini, resulting in very high collagen densities (Fig. 3*E*, green curve). Therefore, the bulk

Downloaded at Palestinian Territory, occupied on December 9, 2021
www.manaraa.com

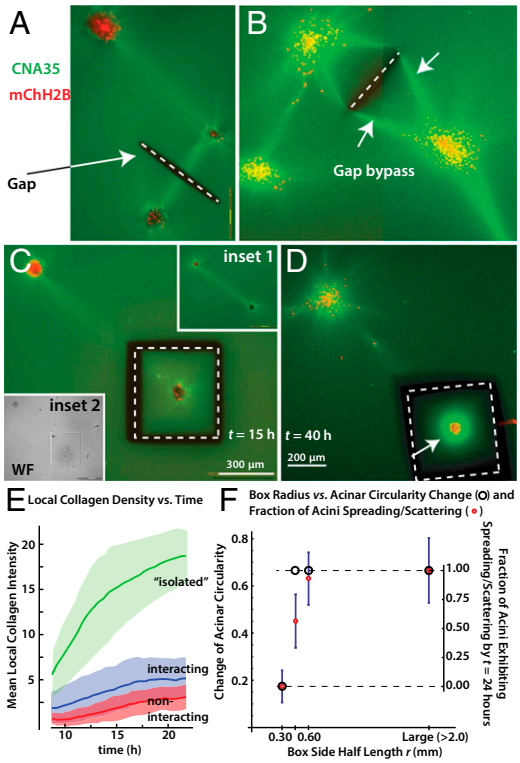

Fig. 3. Mechanical control of transition to invasive phenotype. (*A*) Example of cutting experiment. Acini are allowed to interact and then the collagen line between them is cut (gap = dashed white line). (*B*) Some interacting acini are able to bypass the gap by reconnecting via lines that travel around the gap (white arrows, bypass). The image is a detail of a much larger automated multitile acquisition, similar to Fig. 1 *C* and *D*. (*C*) Example of the box-cut geometry (dashed white line), which isolates an acinus from its neighbors and also the bulk gel. Inset 1, before cutting. Inset 2, immediately after cutting. (*D*) Mechanically isolated acini do not disorganize despite extensive collagen pulling (arrow). (*E*) Mean collagen intensity vs. time for isolated (i.e., box cut as in *C* and *D*), noninteracting, or interacting acini. Observations start at $t = 10$ h due to time needed to move acini from laser cutting microscope to confocal incubator microscope. (*F*) Acinar phenotypes vs. box radius. Acini on the smallest boxes are contractile and can change their circularity slightly over 24 h, but they do not spread or scatter (Movie S13).

collagen density cannot be the primary signal triggering and/or accelerating disorganization, and it is unlikely that the acceleration of acinar disorganization by the lines is mediated simply by increased collagen concentration.

We thus focused our efforts on the substrate stiffness, alignment, and tensile stress, which are all influenced by the size of the collagen cube. Specifically, up to some limit, the stiffness will increase with cube size, and therefore larger cubes will also have higher internal tensile stresses and alignment. We performed additional box-cut experiments with $r > 0.30$ mm, namely, $r = 0.45$ and 0.60 mm. We assessed the acini for spreading/scattering and change of circularity. The latter measure is easier to quantify automatically on our high-throughput imaging system than spreading/scattering but it is harder to interpret because even stable acini undulate/change their circularity slightly over time. Remarkably, when we increased r to 0.45 mm, all acini spread and some even scattered (Fig. 3*F*). There was also a clear loss of circularity, Δc, of −0.45. The loss of circularity was even more pronounced when the box size was increased to 0.60 mm. There, the loss of circularity was indistinguishable from that of acini on bulk collagen ($\Delta c = -0.63$ vs. −0.66), showing that the cube size effect is fully saturated around $r \sim 0.60$ mm. The abrogation of spreading and scattering was not simply due to phototoxicity or hypothetical UV laser–generated factors that block disorganization but not contractility, because acini near the cut but outside of the box still disorganized (Movie S13). The box cutting experiments also rule out potential artifacts that could in principle arise from long-range lateral acini-plastic or vertical acini-glass interactions (*SI Results and Discussion*). Finally, the box-cutting experiments also confirm that the accelerated disorganization we see has a mechanical basis, rather than being mediated by diffusing soluble factors such as TGF-β. A soluble diffusing factor could breach the cuts in the collagen, which would therefore not stop disorganization, unlike what was seen in the experiments. Indeed, separate control experiments in which we completely exchanged the medium four times per hour had no effect on the likelihood or rate of disorganization and the acini extended visible lines between them, as before ($n = 20$ experiments).

In general, the sensitivity of acinar disorganization to cube size can be interpreted in terms of a critical stiffness, a critical tensile stress, a critical alignment, or a combination of these parameters, because as reviewed by Treolar for the simpler but still informative case of rubber (36), the stiffness, tensile stress, and alignment are fundamentally interconnected. However, this does not mean that acini must be equally sensitive to all three parameters. Indeed, inspection of three-acinus systems (Fig. 4) suggests that acini are particularly sensitive to the tensile stresses acting on them. In a typical three-acinus system, two of them interacted creating a collagen line between them, and then, after some delay, the third acinus began to pull collagen. We saw several cases in which the third acinus was able to partially erase the initial collagen line; then, new lines formed as the old line(s) faded. For example, although acinus 2 initially began to protrude toward acinus 3, acinus 2 ultimately disorganized and scattered toward acinus 1, which had the larger collagen pulling rates (Fig. 4, Fig. S7, and Movie S12). As shown in the time traces, acinus 1 began to pull more strongly than acinus 3 at $t = 15.2$ h (arrow, $v_1 > v_3$). In the following 2.6 h ($15.2 < t < 17.8$ h), acinus 2's initial protrusion subsided and a new protrusion, now pointing toward acinus 1, developed (lower trace, arrow, reorientation of main protrusion). Thus, acini are sensitive to substrate mechanics throughout the disorganization process, and distant mechanical changes lead to subtle changes within tens of minutes and in large phenotypic changes within about 3 h.

Over which distances do the mechanical cues extend within the substrate? As quantified by tracking fluorescent beads within the gel, via fluorescent fiducial grids written into the collagen by

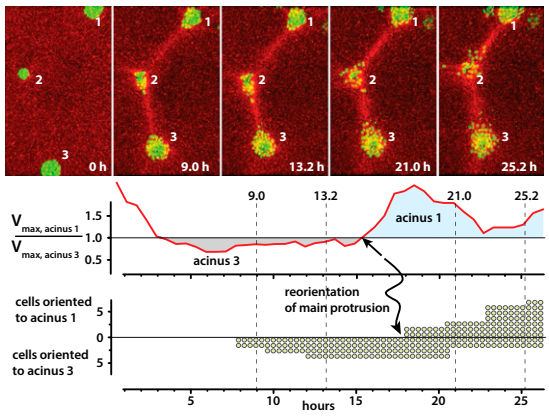

Fig. 4. Mechanical reprogramming of protrusion site and direction. Initially, acinus 3 rapidly pulls collagen, and cells begin to leave acinus 2 toward acinus 3 at $t = 7$ h. Then at $t = 15$ h, acinus 1 begins to pull more rapidly than acinus 3. Ultimately, the middle acinus disorganizes toward acinus 1. Raw velocity maps, image segmentation, and complete movie are shown in Fig. S7 and Movie S12.

BIOPHYSICS AND COMPUTATIONAL BIOLOGY
APPLIED PHYSICAL SCIENCES
Downloaded at Palestinian Territory, occupied on December 9, 2021
www.manaraa.com

localized activation of CNA35-mEos2 or polarization microscopy, acini deformed the collagen over hundreds of micrometers (Figs. S8 and S9 and Movies S14 and 15). Noninteracting acini concentrated and aligned the collagen over distances of at least 550 μm (Fig. S9*B*). When two or more contractile acini were within ∼1.2 mm of one another, lines formed (Fig. S9 *C* and *E–G*), and they extended with little spatial decay over distances of hundreds of micrometers to millimeters (note flat central region of Fig. S9*C*).

We note that that basic mechanical and polymer-physical considerations indicate that the characteristics of the lines, including their length and when and where they will form, will be functions of multiple variables, such as acinar contractility, the strength of cell-cell adhesions, the substrate, and the spatial density and relative arrangement of acini. For example, multicellular structures with reduced cell-cell cohesion would be expected to have impaired ability to form collagen lines. We tested this idea by growing multicellular structures from Michigan Cancer Foundation-7 (MCF-7) cells and then quantifying the extent of line formation and disorganization. The MCF-7 cell line was originally derived from a patient with invasive ductal carcinoma, represents an advanced stage of tumor progression (37, 38), and has further compromised integrity of cell-cell adhesion (39, 40). When grown, extracted, and deposited on collagen 1 like the MCF10AT acini, the MCF-7 spheroids more readily spread, as expected. Although some MCF-7 spheroids were able to form collagen lines (Fig. S9*D*) along which streaming cells then traveled, just as in the MCF10AT experiments, the intense collagen lines were now very rare, with only ∼10% of structures generating a line compared with more than 80% of the MCF10AT acini. Indeed, the majority of MCF-7 spheroids disorganized rapidly without strongly aligning the collagen around them, suggesting that substrate mechanics play a smaller role in their disorganization and/or that MCF-7 spheroids have a smaller critical tension/alignment needed to trigger disorganization.

We then turned our attention to the motile cells that were leaving the acini along the collagen lines formed by the MCF10AT acini. The single cells' motility and morphology, including their long and thin projections, were reminiscent of mesenchymal cells, raising the possibility of an epithelial-to-mesenchymal transition (EMT). We used immuno-fluorescence mapping of intact acini and single cells streaming from disorganizing acini to quantify the levels and subcellular distributions of three classic EMT markers: E-cadherin, β-catenin, and vimentin (Fig. 5 *A–D*). A primary step in acinar disorganization and appearance of motile single cells is the weakening of cell-cell junctions through reduction of E-cadherin levels (41) and the loss of cytoplasmic β-catenin. Although E-cadherin is a hallmark of the epithelial cell state, the intermediate filament protein vimentin is selectively up-regulated in mesenchymal cells (42). A combination of high vimentin, changes in the levels and/or location of E-cadherin and β-catenin, and accelerated mobility of disseminating cells have been equated with an EMT (43). As shown in Fig. 5 *A–D*, the cells at the top and the sides of the acini had the expected epithelial signatures, including high levels of E-cadherin and β-catenin and low or no vimentin. By contrast, cells at the collagen/acinus interface, especially the single migratory cells on the collagen lines, had reduced E-cadherin and β-catenin but high vimentin (Fig. 5*B*). Together with the phenotypic changes, the molecular changes in the cells at the collagen/acinus boundary and in the streaming cells are consistent with the possibility of an EMT occurring as the cells leave their parent acinus and travel along the collagen lines. Additional work, especially studies of the dynamics and reversibility of the transition, will be needed to formally prove a classical EMT.

How might cells at the substrate-acinus interface sense mechanical cues and what might those cues be? The collagen lines resisted lateral deformation by an atomic force microscope (AFM) cantilever eightfold more than unaligned control regions

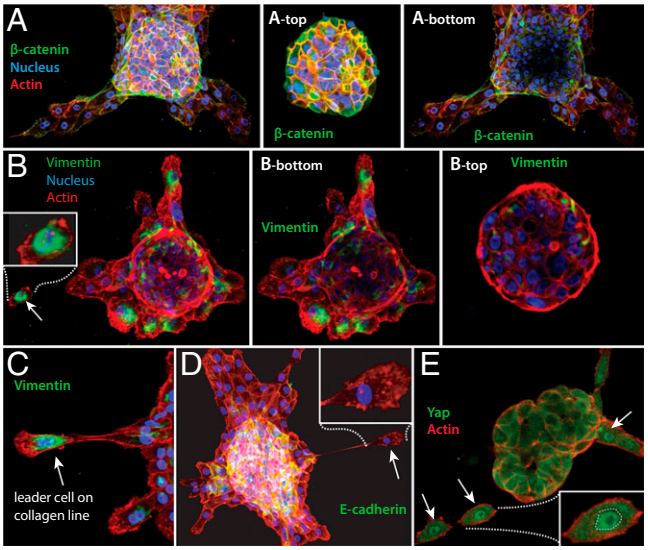

Fig. 5. Expression changes during acinar disorganization. (*A*) Cells toward the top of the acinus have robust β-catenin expression (*Upper*), unlike cells toward the bottom of the acinus and in direct contact with collagen (*Lower*). (*B*) The opposite pattern is seen with the mesenchymal marker Vimentin. Individual cells in contact with and spreading on the collagen have high Vimentin (*Lower*) unlike the majority of cells at the top of the acinus (*Upper*). (*C*) Leader cells leaving the acini along collagen lines have prominent perinuclear Vimentin and mesenchymal cell architecture. (*D*) Cells at the acinus/collagen interface have lost E-cadherin. (*Inset*) Zoom of a pioneer migratory cell on collagen line with no detectable E-cadherin. (*E*) Cells leaving acini along lines sense a stiffened environment as judged by nuclear relocation of the YAP mechanosensory protein (white arrows).

(Fig. S10 *A–E*), suggesting that the lines were mechanically loaded by contractile acini at either end. Cells leaving the acini along lines had nuclear localization of the Yap/Taz mechano-transducer (44), indicating tension on the cells' actomyosin cytoskeleton (Fig. 5*E*, Fig. S10, and Movie S16) and showing that the cells were sensing the altered environment.

The phenomena reported here constitute a collective biological signaling mechanism where the polymer-physical properties of the extracellular material are fundamental to signal generation and its spatial propagation and duration. When two or more contractile acini are within a material's dependent distance (in our conditions, typically ∼1.2 mm) of one another, their collagen pulling fields overlap; lines then form and mechanically interconnect the acini. It is already known that acini disorganize in a dose-dependent manner on inappropriately hard matrices (11). Here, the acini themselves mechanically remodel the matrix, resulting in several fundamentally connected changes within the gel (tensile stresses; alignment; and directional stiffening), which then drive and coordinate changes in acinar behavior, morphology, and protein localization (Fig. S11). One simple explanation for our observations is that the decision of an acinus to transition to an invasive phenotype is significantly influenced by the magnitude of the tensile stress acting on it and that there is a threshold beyond which tensile stress drives a malignant transformation, although a response to collagen alignment is also compatible with all observations. The relative contributions of collagen alignment and the tensile stress to disorganization remain unclear and await further study. The possible importance of the tensile stress in our system is consistent with the broader mechanobiology literature, such as the finding that scattering of epithelial cell monolayers is regulated by integrin-dependent actomyosin contraction (30). Interestingly, the box-cut experiments show that spreading/scattering can be entirely blocked by suitable mechanical intervention (Fig. 3), whereas small

Downloaded at Palestinian Territory, occupied on December 9, 2021
www.manaraa.com

molecule inhibition of actomyosin contractility and Rho-ROCK signaling reduces but does not entirely block spreading/scattering (Fig. S3). Therefore, there must exist at least one more presently unknown mechanosensitive mechanism for acinar transition to an invasive phenotype, which awaits further study.

Methods

A detailed description of methods and materials is given in the *SI Methods*. Briefly, cell line maintenance, acini preparation, and immunostaining followed standard protocols (28, 45). Collagen gels were prepared according to the manufacturer's instructions. Acini were isolated from Matrigel using ice-cold Tris buffer/EDTA (45). The CNA35 collagen binding protein cDNA (a gift of Magnus Hook, Texas A&M University, College Station, TX) was inserted into a pET *Escherichia coli* expression vector carrying an N-terminal 6X his and a C-terminal mEos2 or EGFP, and the protein was expressed, purified, and added to the collagen gels to visualize collagen. Collagen was cut with a Zeiss Microbeam system. Acinar and substrate dynamics were monitored using laser scanning confocal (Zeiss LSM 700, Zeiss LSM 780), widefield fluorescence (MetaXpress, CIRM/QB3 facility at UC Berkeley), polarization microscopy, SEM, and AFM. Data were analyzed with custom Matlab scripts or Imaris (Bitplane), PIVlab, or ImageJ.

ACKNOWLEDGMENTS. We thank Robert I. Saye (Mathematics Department, University of California, Berkeley) for comments and suggestions. We thank the anonymous reviewers for numerous excellent suggestions, including comparing MCF-10AT acini to MCF-7 spheroids and the immuno-fluorescence study of cells streaming from their parent acini. We thank Shelley Hwang, MD, MPH (Duke University), for extensive discussions and suggestions. This work was partially supported by the National Institutes of Health (NIH) Grant GM77856 (to J.T.L.) and NIH/National Cancer Institute (NCI) Grants U54CA143836 (to J.T.L.) and R01CA138818 (to V.M.W.), the Applied Mathematical Science subprogram of the Office of Energy Research, US Department of Energy Contract DE-AC02-05CH11231, and the Division of Mathematical Sciences of the National Science Foundation. J.A.S. was supported by the Miller Foundation at University of California, Berkeley and as an Einstein Visiting Fellow of the Einstein Foundation (Berlin).

1. Chen CS, Mrksich M, Huang S, Whitesides GM, Ingber DE (1997) Geometric control of cell life and death. *Science* 276(5317):1425–1428.
2. Rauzi M, Lecuit T (2009) Closing in on mechanisms of tissue morphogenesis. *Cell* 137(7):1183–1185.
3. Engler AJ, Sen S, Sweeney HL, Discher DE (2006) Matrix elasticity directs stem cell lineage specification. *Cell* 126(4):677–689.
4. Ingber DE (2006) Cellular mechanotransduction: Putting all the pieces together again. *FASEB J* 20(7):811–827.
5. Nelson CM, et al. (2005) Emergent patterns of growth controlled by multicellular form and mechanics. *Proc Natl Acad Sci USA* 102(33):11594–11599.
6. Provenzano PP, Inman DR, Eliceiri KW, Trier SM, Keely PJ (2008) Contact guidance mediated three-dimensional cell migration is regulated by Rho/ROCK-dependent matrix reorganization. *Biophys J* 95(11):5374–5384.
7. Provenzano PP, Inman DR, Eliceiri KW, Keely PJ (2009) Matrix density-induced mechanoregulation of breast cell phenotype, signaling and gene expression through a FAK-ERK linkage. *Oncogene* 28(49):4326–4343.
8. Guo CL, et al. (2012) Long-range mechanical force enables self-assembly of epithelial tubular patterns. *Proc Natl Acad Sci USA* 109(15):5576–5582.
9. Discher DE, Janmey P, Wang YL (2005) Tissue cells feel and respond to the stiffness of their substrate. *Science* 310(5751):1139–1143.
10. Vader D, Kabla A, Weitz D, Mahadevan L (2009) Strain-induced alignment in collagen gels. *PLoS ONE* 4(6):e5902.
11. Paszek MJ, et al. (2005) Tensional homeostasis and the malignant phenotype. *Cancer Cell* 8(3):241–254.
12. Levayer R, Lecuit T (2012) Biomechanical regulation of contractility: Spatial control and dynamics. *Trends Cell Biol* 22(2):61–81.
13. Sun Y, Chen CS, Fu J (2012) Forcing stem cells to behave: A biophysical perspective of the cellular microenvironment. *Annu Rev Biophys* 41:519–542.
14. Fernandez P, Bausch AR (2009) The compaction of gels by cells: A case of collective mechanical activity. *Integr Biol (Camb)* 1(3):252–259.
15. Arnaout MA, Goodman SL, Xiong JP (2007) Structure and mechanics of integrin-based cell adhesion. *Curr Opin Cell Biol* 19(5):495–507.
16. Schwartz MA, Ginsberg MH (2002) Networks and crosstalk: Integrin signalling spreads. *Nat Cell Biol* 4(4):E65–E68.
17. Margadant C, Sonnenberg A (2010) Integrin-TGF-beta crosstalk in fibrosis, cancer and wound healing. *EMBO Rep* 11(2):97–105.
18. Shergill B, Meloty-Kapella L, Musse AA, Weinmaster G, Botvinick E (2012) Optical tweezers studies on Notch: Single-molecule interaction strength is independent of ligand endocytosis. *Dev Cell* 22(6):1313–1320.
19. Wang XF, Ha T (2013) Defining single molecular forces required to activate integrin and notch signaling. *Science* 340(6135):991–994.
20. Sawhney RK, Howard J (2002) Slow local movements of collagen fibers by fibroblasts drive the rapid global self-organization of collagen gels. *J Cell Biol* 157(6):1083–1091.
21. Dhimolea E, Maffini MV, Soto AM, Sonnenschein C (2010) The role of collagen reorganization on mammary epithelial morphogenesis in a 3D culture model. *Biomaterials* 31(13):3622–3630.
22. Conklin MW, et al. (2011) Aligned collagen is a prognostic signature for survival in human breast carcinoma. *Am J Pathol* 178(3):1221–1232.
23. Levental KR, et al. (2009) Matrix crosslinking forces tumor progression by enhancing integrin signaling. *Cell* 139(5):891–906.
24. Bondareva A, et al. (2009) The lysyl oxidase inhibitor, beta-aminopropionitrile, diminishes the metastatic colonization potential of circulating breast cancer cells. *PLoS ONE* 4(5):e5620.
25. Wellings SR, Jensen HM, Marcum RG (1975) An atlas of subgross pathology of the human breast with special reference to possible precancerous lesions. *J Natl Cancer Inst* 55(2):231–273.
26. Parsons BL, Meng F (2009) K-RAS mutation in the screening, prognosis and treatment of cancer. *Biomarkers Med* 3(6):757–769.
27. Wang F, et al. (1998) Reciprocal interactions between beta1-integrin and epidermal growth factor receptor in three-dimensional basement membrane breast cultures: A different perspective in epithelial biology. *Proc Natl Acad Sci USA* 95(25):14821–14826.
28. Debnath J, Muthuswamy SK, Brugge JS (2003) Morphogenesis and oncogenesis of MCF-10A mammary epithelial acini grown in three-dimensional basement membrane cultures. *Methods* 30(3):256–268.
29. Borghi N, Lowndes M, Maruthamuthu V, Gardel ML, Nelson WJ (2010) Regulation of cell motile behavior by crosstalk between cadherin- and integrin-mediated adhesions. *Proc Natl Acad Sci USA* 107(30):13324–13329.
30. de Rooij J, Kerstens A, Danuser G, Schwartz MA, Waterman-Storer CM (2005) Integrin-dependent actomyosin contraction regulates epithelial cell scattering. *J Cell Biol* 171(1):153–164.
31. Uehata M, et al. (1997) Calcium sensitization of smooth muscle mediated by a Rho-associated protein kinase in hypertension. *Nature* 389(6654):990–994.
32. Limouze J, Straight AF, Mitchison T, Sellers JR (2004) Specificity of blebbistatin, an inhibitor of myosin II. *J Muscle Res Cell Motil* 25(4-5):337–341.
33. Straight AF, et al. (2003) Dissecting temporal and spatial control of cytokinesis with a myosin II Inhibitor. *Science* 299(5613):1743–1747.
34. Kiehart DP, Galbraith CG, Edwards KA, Rickoll WL, Montague RA (2000) Multiple forces contribute to cell sheet morphogenesis for dorsal closure in Drosophila. *J Cell Biol* 149(2):471–490.
35. Kiehart DP, et al. (2006) *Ultraviolet Laser Microbeam for Dissection of Drosophila Embryos Cell Biology: A Laboratory Handbook* (Elsevier Science, Amsterdam), pp 87–103.
36. Treloar LRG (1973) The elasticity and related properties of rubbers. *Rep Prog Phys* 36(7):755.
37. Heppner GH, Miller FR, Shekhar PM (2000) Nontransgenic models of breast cancer. *Breast Cancer Res* 2(5):331–334.
38. Chandler EM, et al. (2012) Implanted adipose progenitor cells as physicochemical regulators of breast cancer. *Proc Natl Acad Sci USA* 109(25):9786–9791.
39. Neve RM, et al. (2006) A collection of breast cancer cell lines for the study of functionally distinct cancer subtypes. *Cancer Cell* 10(6):515–527.
40. Fang X, et al. (2011) Twist2 contributes to breast cancer progression by promoting an epithelial-mesenchymal transition and cancer stem-like cell self-renewal. *Oncogene* 30(47):4707–4720.
41. Zheng H, Kang Y (2013) Multilayer control of the EMT master regulators. *Oncogene*, 10.1038/onc.2013.128.
42. Kokkinos MI, et al. (2007) Vimentin and epithelial-mesenchymal transition in human breast cancer—Observations in vitro and in vivo. *Cells Tissues Organs* 185(1-3):191–203.
43. Gilles C, Thompson EW (1996) The epithelial to mesenchymal transition and metastatic progression in carcinoma. *Breast J* 2(1):83–96.
44. Dupont S, et al. (2011) Role of YAP/TAZ in mechanotransduction. *Nature* 474(7350):179–183.
45. Lee GY, Kenny PA, Lee EH, Bissell MJ (2007) Three-dimensional culture models of normal and malignant breast epithelial cells. *Nat Methods* 4(4):359–365.

Downloaded at Palestinian Territory, occupied on December 9, 2021

www.manaraa.com